Tellus
SERIES B
CHEMICAL
AND PHYSICAL
METEOROLOGY
PUBLISHED BY THE INTERNATIONAL METEOROLOGICAL INSTITUTE IN STOCKHOLM

Tellus (2011), 63B, 328–339
Printed in Singapore. All rights reserved

TELLUS

Regional trends in terrestrial carbon exchange and their seasonal signatures

By KEVIN R. GURNEY[1]* and WARREN J. ECKELS[2], [1]*School of Life Sciences, Arizona State University, PO Box 874501, Tempe, AZ 85287-4501, USA;* [2]*Department of Earth and Atmospheric Sciences, Purdue University, 550 Stadium Mall Drive, West Lafayette, IN 47906, USA*

(Manuscript received 15 October 2010; in final form 29 March 2011)

ABSTRACT

The trends of terrestrial carbon exchange and their mechanistic drivers are key components in understanding how carbon reservoirs will respond to climate change. Here we show trends in seasonal non-fossil land–atmosphere carbon exchange from 1980 to 2008 using atmospheric CO_2 inversion results. Four indices were analysed: growing-season net flux (GSNF), dormant-season net flux (DSNF), amplitude and annual net carbon flux (NCF). We find that the global land carbon sink is intensifying at -0.057 ± 0.01 PgC yr^{-2}, resulting in -1.65 ± 0.29 PgC of additional uptake over the period examined. This increased total land uptake is driven by a decline in the DSNF (-0.04 ± 0.01 PgC yr^{-2}) and intensification of the GSNF (-0.02 ± 0.008 PgC yr^{-2}). Regional analysis shows the dominant role of the southern half of the African continent; intensification of the GSNF (-0.02 ± 0.005 PgC yr^{-2}) and a decline in the DSNF (-0.013 ± 0.004 PgC yr^{-2}) imply that Africa has shifted from a net carbon source in the 1980s to near-neutral emissions. By contrast, a weakening of the GSNF is found in temperate North America (0.015 ± 0.007 PgC yr^{-2}) and tropical America (0.01 ± 0.005 PgC yr^{-2}).

1. Introduction

The emission of fossil fuel CO_2 to the Earth's atmosphere is moderated by carbon uptake in the terrestrial biosphere and oceans, removing slightly more than half of annual fossil fuel and land-use change carbon emissions (Canadell et al., 2007). Recent syntheses indicate that the terrestrial global carbon sink removed -1.7 PgC yr^{-1} (range: -3.4 to $+0.2$ PgC yr^{-1}) and -2.6 PgC yr^{-1} (range: -4.3 to -0.9 PgC yr^{-1}), for the decade of the 1980s and 1990s, respectively (Denman et al., 2007). The ocean removal has been estimated at -1.8 PgC yr^{-1} (± 0.8) and -2.2 PgC yr^{-1} (± 0.4) for the 1980s and 1990s, respectively. The ability of the land and oceans to continue removing the additional burden of atmospheric CO_2, however, is poorly understood (Le Quere et al., 2009). Recent work has shown that projections of atmospheric CO_2 concentrations and the resulting climate change rely to a significant degree on projections about future land and ocean uptake (Friedlingstein et al., 2006; Sitch et al., 2008).

Though the land and ocean uptake exhibit considerable year-to-year variability (Gurney et al., 2008), the presence of a secular trend in recent decades, particularly at the regional to continental scale, may offer insight into the future behaviour of this CO_2 removal. Because the terrestrial surface is directly and indirectly influenced by human activity and hypothesized to have a potential for large-scale climate-carbon feedbacks, the terrestrial uptake is of particular interest (Cox et al., 2000).

A number of studies have attempted to quantify trends in terrestrial net carbon exchange. Some have utilized terrestrial biosphere models, driven variously by climate, CO_2 and land-use change data sets (Cao et al., 2002; Potter et al., 2003; Le Quere et al., 2009; Piao et al., 2009). However, uncertainty in the underlying drivers and model uncertainties result in a large spread of results. Others rely on partially or indirectly observed measures such as NDVI and sampled NPP (Myneni et al., 1997; Schaefer et al., 2002; Nemani et al., 2003; Goetz et al., 2005; Lopatin et al., 2006; Lewis et al., 2009). Translating these indices into a net carbon exchange, however, remains challenging. Finally, some studies have assessed the trend in the airborne fraction of CO_2, which reflect the efficiency with which land and ocean uptake operate (Raupach et al., 2008; Le Quere et al., 2009). However, trends in the airborne fraction face a couple of difficulties. First, they rely on estimates of land-use change emissions, which remain highly uncertain relative to the other two elements of the airborne fraction calculation, fossil fuel emissions and the atmospheric CO_2 growth rate (Knorr 2009).

*Corresponding author.
e-mail: kevin.gurney@asu.edu
DOI: 10.1111/j.1600-0889.2011.00534.x

Secondly, any variations in the growth in fossil fuel or land use change from a smooth exponential path is reflected in the calculated AF (airborne fraction) and its trend, making interpretation of trends in the AF difficult (Gloor et al., 2010).

An alternative approach is to utilize the results of atmospheric CO_2 inversions, constrained by observed atmospheric CO_2 concentration (Tans et al., 1990) and simulated atmospheric transport, to estimate trends in the estimated flux (Enting, 2002). By isolating different components of each year's net flux, inverse results can be used to shed light on mechanistic information. This paper reports on such trend estimation at spatial scales down to the continents using the results of the TransCom 3 international atmospheric CO_2 inversion intercomparison (Gurney et al., 2002, 2008). In order to decompose the trends of net carbon exchange into seasonal representations, four different carbon exchange indices were created. The trends in these indices are analysed in the context of regional climate drivers to inform future carbon cycle dynamics and fill gaps in knowledge regarding regional net carbon exchange.

2. Methods

2.1. Inverse results

Monthly net carbon exchange for the 11 land regions defined in the TransCom 3, Level 2 experiment over the 1980–2008 time period were obtained from an inversion constrained by a network of 23 CO_2 observing stations (Gurney et al., 2008; GlobalView, 2009). The flux estimates reflect total net exchange with the land and ocean beyond the fossil fuel CO_2 flux. A land region is defined here as a region of continental scale with relatively homogeneous vegetation and climate. A map of the land regions and a discussion of regional definitions appears in Gurney et al. (2003).

The inversion approach used in this study follows the Bayesian synthesis method (Enting, 2002). The goal of the atmospheric inversion process is to find the optimal combination of regional surface net carbon fluxes (NCFs), $\vec{S}$, that best matches observed CO_2, $\vec{D}$, after those fluxes have been transported through a model atmosphere represented by the operator, $\boldsymbol{M}$. This is most succinctly represented by the minimization of cost function, J.

$$J = \frac{1}{2}\Big[(M\vec{S} - \vec{D})^T C(\vec{D})^{-1}(M\vec{S} - \vec{D}) + (\vec{S} - \vec{S}_0)^T C(\vec{S}_0)^{-1}(\vec{S} - \vec{S}_0)\Big], \quad (1)$$

where $C(\vec{D})$ embodies confidence in the form of an error or uncertainty covariance on the mismatch between modelled and observed concentration, and $C(\vec{S})$ represents the prior uncertainty covariance on the prior fluxes. The regional prior fluxes are the same as those employed in the earlier TransCom 3 cyclostationary inversion and were determined from independent estimates of terrestrial and oceanic exchange. The land region prior flux estimates incorporate results from recent inventory studies and are identical to the annual mean values used in the annual mean inversion (Gurney et al., 2003). Because the land region prior fluxes are only available as annual mean values, these were distributed evenly over those months considered the most likely to capture the emission or uptake implied by the prior flux (i.e. extratropical uptake placed into the growing season, tropical emissions placed into the dry season, Gurney et al., 2004). The ocean region prior flux estimates were prescribed as zero for each month. Neither prior flux contained a temporal trend. A detailed description of the formalism employed and references to source material is given in previous work (Gurney et al., 2003, 2004; 2008; Baker et al., 2006).

Flux uncertainty in atmospheric inversions derives from a variety of sources including transport, flux boundary conditions [represented by $C(\vec{S})$], atmospheric CO_2 measurements and representation error (Engelen et al., 2002). Representation error can be divided into an internal and external error. Internal error arises from differences in the spatial resolution of the transport model versus the resolution at which the fluxes are solved. External representation uncertainty arises from the mismatch between an atmospheric measurement and a simulated representation of that measurement in space and time.

All of these uncertainties, other than the error on the prior flux estimates, are incorporated into the model-data mismatch error covariance matrix, $C(\vec{D})$. Much of this uncertainty is represented by an estimate of the signal to noise at a measurement location (Baker et al., 2006).

For the prior flux uncertainty on land in a given month we chose the combination of the uncertainties employed in our annual mean control case (Gurney et al., 2002), and 30% each of NPP and respiration provided by the CASA model of net ecosystem production (Randerson et al., 1997). Since it is unlikely that a given region/month flux adjustment would exceed these values, this provides a reasonable, ecologically relevant upper bound.

The regional ocean prior flux uncertainties for each month are a constant value defined as

$$C(\vec{S}_{\mathrm{ocn}}) = \sqrt{(0.5\,\mathrm{GtC\ yr^{-1}})^2 + [C(\vec{S}_{L1,\mathrm{ocn}})]^2}, \quad (2)$$

where $C(\vec{S}_{L1,\mathrm{ocn}})$ are the annual mean prior flux uncertainties used in the annual mean control inversion (Gurney et al., 2002).

In order to ensure that the trends calculated are not sensitive to the relatively tight ocean prior flux uncertainties used in the TransCom 3 inversion intercomparison (Gurney et al., 2008), the analysis was repeated with ocean prior flux uncertainties increased by a factor of 3 (not shown). The primary difference is the loss of statistical significance in the aggregate region results, notably the northern land and tropical land aggregates. No instances of a trend sign change occur as a results of the looser ocean priors.

Each month's net carbon exchange in the 1980–2008 time period was analysed across the 13 participating transport models to identify outliers. For every month, the model mean carbon exchange, μ, and a population standard deviation, σ, of the monthly carbon exchange reported by each model was determined. Any model-month's reported carbon flux that was outside the range $(\mu - 3\sigma, \mu + 3\sigma)$ was defined as an outlier and removed, then the intermodel mean was recalculated. A priori deletions of spurious data during the winter were considered, but rejected: while it can be safely stated that the northern boreal land regions experience little net uptake of carbon dioxide in January, such knowledge of the behaviour of all regions every month was lacking. Fewer than 1% of monthly carbon exchange values were discarded.

2.2. *Flux indices*

The monthly fluxes for each of the 13 transport models were aggregated to produce the four aggregate indicators of the non-fossil fuel component of net carbon exchange (Fig. 1): growing season net flux (GSNF), dormant season net flux (DSNF), amplitude (AMP = |DSNF – GSNF|) and net carbon flux (NCF = DSNF + GSNF). These indices were defined for each of the 29 yr and each of the 13 transport models. It is important to note that the inverse-estimated net carbon exchange includes land-use change fluxes such as deforestation or fire emissions within the estimated flux.

GSNF, DSNF, AMP and NCF are defined to isolate different seasonal contributions to the non-fossil fuel net carbon exchange in the terrestrial regions. The growing season is defined as every month within a year that non-fossil fuel net carbon exchange is negative, that is, the region acts as a net carbon sink during those months. The dormant season is defined as every month within a year that non-fossil fuel net carbon exchange is a positive value implying that the land region is a net carbon source during those months. A negative NCF indicates an annual total net carbon sink; a positive NCF indicates an annual total net carbon source. A negative trend in the NCF can imply either a declining source or an increasing sink, depending upon the absolute magnitude of the regional NCF.

In all cases, monthly carbon exchange was defined as 1/12 the reported annual flux value, which changes the units from PgC yr^{-1} to PgC $month^{-1}$ (see Fig. 1) in order to compute the index values. Each month was represented by one data point from each model.

In order to account for the impact of autocorrelation in the individual model monthly time series, an autoregression with a lag of 1 month was performed. The effective sample size is estimated using the relationship outlined in Bretherton

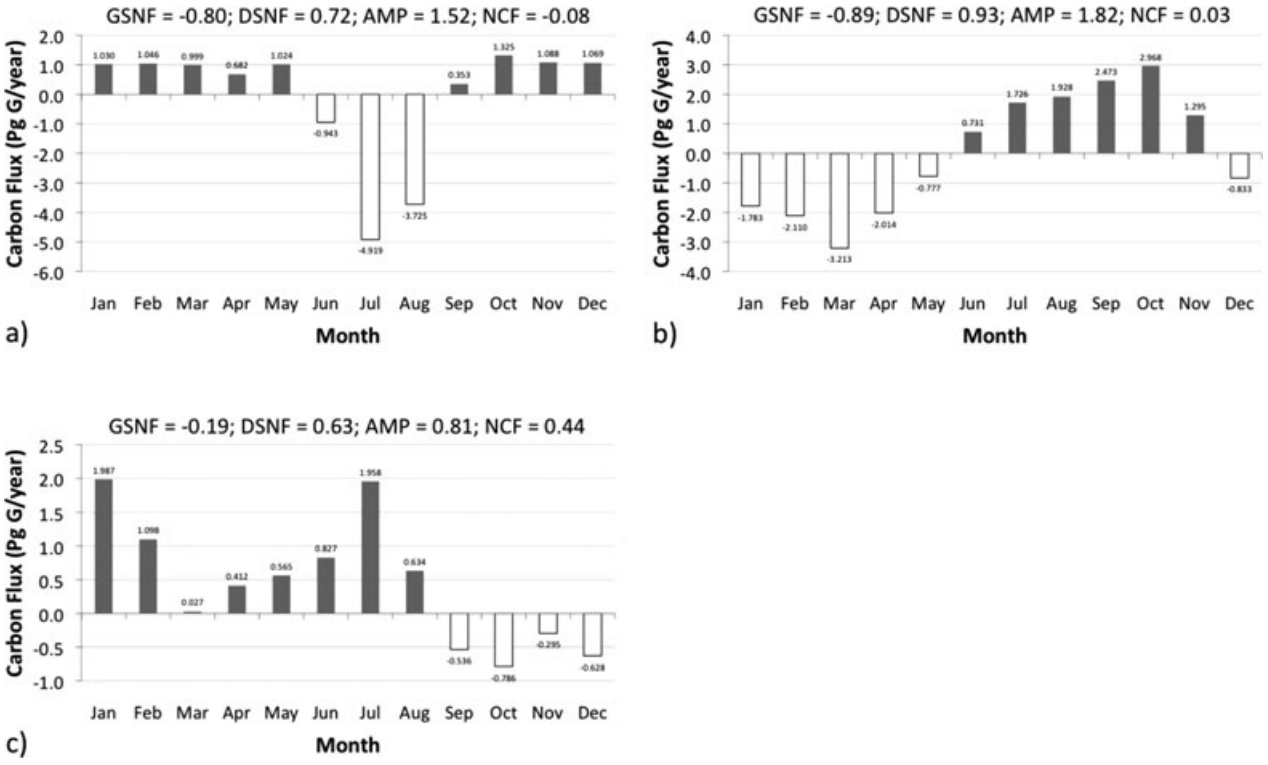

Fig. 1. A demonstration of how carbon flux indices [GSNF, growing season net flux; DSNF, dormant season net flux; AMP, amplitude (|DSNF – GSNF|); NCF, net carbon flux (GSNF + DSNF)] are calculated. Any month for which the net carbon flux is negative is included in the GSNF (open vertical bars). Any month for which the net carbon flux is positive is included in the DSNF (filled vertical bars). Mean 2000–2008 fluxes shown for boreal North America (a) southern Africa (b) and tropical Asia (c).

et al. (1999).

$$N_{\text{eff}} = N\frac{1 - r_1 r_2}{1 + r_1 r_2}, \quad (3)$$

where N_{eff} is the effective sample size; N is the sample size; and r_1 and r_2 are the lag-one autocorrelations of the time series being correlated. The actual degrees of freedom ranged from 300 to 336.

A reduction in the degrees of freedom results in wider confidence limits on the trend coefficient, and a trend must be more clearly positive or negative in order to be safely distinguished from random noise. This precaution carried out, it was determined that the lowest number of degrees of freedom obtained was 144. The Student's t distributions for $N = 144$ and $N = 336$ differ little from the normal distribution, so autocorrelation was not considered.

A regression was performed on the time series of each index. These four time series (corresponding to the four indices) is composed of 29 annual values, each annual value is represented by a cloud of 13 values (one for each participating model). The trend for each index was deemed significant if the slopes of the upper and lower 95% confidence limits were the same sign, that is, if there is a probability of at least 0.95 that the direction of the trend determined by linear regression is correctly chosen.

To utilize the monthly model posterior uncertainties in assessing the significance of the index trends, a Monte Carlo analysis with 1000 members was performed on the estimated fluxes. For each model and month, the mean μ and the posterior uncertainty σ of the model estimated flux was used to create an N(μ, σ^2) distribution. Using the Box–Muller transform, two numbers randomly generated from U(0,1) were mapped into N(μ, σ^2) (Box and Muller, 1958). As before, the intermodel mean and population standard deviation of these perturbed values was calculated, and individual model-months were deleted if they were deemed outliers, that is, more than three standard deviations away from the intermodel mean.

From the 1000 perturbed monthly data sets generated by this method, the four aggregates (GSNF, DSNF, AMP and NCF) were determined for each calendar year and a linear regression performed upon them. The slopes of each regression were ranked from highest to lowest. The 26th highest slope was deemed the upper 95% confidence limit while the 975th highest slope was determined the lower 95% confidence limit. Again, a trend was deemed significant if slopes of the upper and lower confidence limits both carried the same sign.

If the trend of a land region's index (GSNF, DSNF, AMP and NCF) was determined significant both through the calculation of a 95% confidence bound for the line of regression and through the Monte Carlo analysis, the index trend was deemed statistically significant. This approach attempts to ensure that the significance of the index slope reflects not only the spread due to model-to-model differences, but the uncertainty associated with each model's individual estimate.

The change in each index from 1980 to 2008 was estimated by multiplying the slope by 29. A confidence interval for this change was also obtained by multiplying the confidence interval by 29 to obtain a confidence interval for the entire period. This method almost certainly leads to an overestimation of the error interval, since it assumes that every year's data are a linear combination of every other year's data, which is unlikely.

2.3. *Caveats*

A number of caveats are worth noting. First, the inverse results were generated by models in which no interannually varying transport was present. Hence, modellers chose a particular calendar year of transport winds and recycled those across the years of simulation. Though each modelling group utilized a different chosen year for their recycled transport, it is not clear what impact this choice has on the results presented here. The influence within inverse studies of interannually varying transport versus interannually varying fluxes on atmospheric CO_2 remains inconclusive though the balance of evidence suggests that interannually varying transport is of secondary importance (Rödenbeck et al., 2003; Peylin et al., 2005; Piao et al., 2008).

The study assumes the fossil fuel fluxes as a fixed known with no associated uncertainty. Hence, any bias in the fossil fuel flux trends will be aliased into the non-fossil trends estimated here.

This study utilizes an observing network of 23 CO_2 observing stations and hence, has a limited observational constraint lacking observations in many large portions of the planet. However, as established in a recent study, the sensitivity of the inverse results to increasing the size of the observational network is primarily reflected in estimation of the long-term means and not on interannual variability or trends (Gurney et al., 2008). However, a larger observing network would undoubtedly lower the trend uncertainty presented here.

3. Results and discussion

The regional flux index trends, regional aggregated trends, decadal long-term means and associated uncertainties are shown in Table 1. The three decades are 1980–1989 (inclusive), 1990–1999 (inclusive) and 2000–2008 (inclusive). Observational CO_2 data were not available for 2009 hence, the decadal mean for the current decade includes fluxes up to the end of 2008 only.

Previous analysis has shown that a particular subset of the 13 TransCom 3 models might better represent near-surface vertical transport and hence, may offer a better estimate of inverse-estimated fluxes (Stephens et al., 2007). This was accomplished by comparing predicted CO_2 vertical profiles at a series of sites not utilized as an observational constraint in the transport inversion. This does not guarantee that the three identified models have correct transport (a challenge when using only CO_2 observations) but that these three may be closer to correct transport

Table 1. TransCom 3 model mean carbon exchange index trends and 95% confidence intervals for the 1980–2008 time period and decadal mean net exchange for the individual land regions and regional aggregates

Region or regional aggregate	GSNF (PgC yr^{-2})	DSNF (PgC yr^{-2})	AMP (PgC yr^{-2})	NCF (PgC yr^{-2})	Long-term average NCF (PgC yr^{-1}) & total uncertainty (1s)		
					1980–1989	1990–1999	2000–2008
Boreal N America	-0.011 ± 0.002	NS	0.011 ± 0.004	-0.012 ± 0.004	0.15 (0.34)	−0.01 (0.32)	−0.09 (0.33)
Temperate N America	0.015 ± 0.007	NS	-0.020 ± 0.010	0.012 ± 0.008	−1.12 (0.39)	−0.58 (0.37)	−0.86 (0.39)
Tropical America	0.010 ± 0.005	0.010 ± 0.005	NS	0.020 ± 0.008	−0.18 (0.54)	−0.05 (0.58)	0.21 (0.60)
South America	-0.011 ± 0.003	-0.007 ± 0.003	NS	-0.018 ± 0.005	0.23 (0.33)	0.12 (0.33)	−0.10 (0.33)
Northern Africa	0.003 ± 0.002	-0.006 ± 0.003	-0.009 ± 0.003	NS	0.02 (0.35)	−0.10 (0.36)	−0.06 (0.39)
Southern Africa	-0.020 ± 0.005	-0.013 ± 0.004	NS	-0.032 ± 0.008	0.64 (0.58)	−0.12 (0.56)	0.04 (0.62)
Boreal Asia	-0.014 ± 0.004	NS	0.014 ± 0.008	-0.013 ± 0.007	−0.15 (0.55)	−0.44 (0.49)	−0.37 (0.50)
Temperate Asia	NS	NS	NS	NS	0.00 (0.38)	−0.02 (0.36)	−0.07 (0.36)
Tropical Asia	NS	NS	NS	NS	0.51 (0.30)	0.37 (0.32)	0.44 (0.31)
Australasia	-0.003 ± 0.002	-0.003 ± 0.001	NS	-0.006 ± 0.002	−0.17 (0.11)	−0.09 (0.09)	−0.34 (0.12)
Europe	NS	NS	NS	NS	−1.00 (0.24)	−0.74 (0.29)	−1.14 (0.28)
Northern Land	-0.009 ± 0.007	NS	NS	-0.016 ± 0.010	−2.10 (0.63)	−1.80 (0.60)	−2.53 (0.58)
Tropical Land	0.013 ± 0.006	NS	-0.012 ± 0.008	0.015 ± 0.012	0.34 (0.77)	0.22 (0.82)	0.59 (0.84)
Southern Land	-0.035 ± 0.007	-0.021 ± 0.005	NS	-0.056 ± 0.009	0.71 (0.58)	−0.09 (0.60)	−0.40 (0.60)
Total Land	-0.020 ± 0.008	-0.037 ± 0.011	NS	-0.057 ± 0.014	−1.10 (0.48)	−1.66 (0.51)	−2.34 (0.56)

Notes: Uncertainties associated with the long-term decadal means reflect the quadrature sum of the 1σ model spread and the 1σ RMS of the individual posterior uncertainty.
Details of the uncertainty estimation on the long-term averages can be found in previous reports (Gurney et al., 2003).
GSNF, growing season net flux; DSNF, dormant season net flux; AMP, amplitude (|DSNF – GSNF|); NCF, net carbon flux (GSNF+DSNF).

out of the large 13-model suite. Estimate of the long-term mean fluxes do differ between the mean of all 13 models and the three identified in Stephens et al. (2007) but the trends are nearly identical. Some of this agreement is, no doubt, due to the fact that the participating models did not run differing interannually varying winds. However, the agreement suggests that the trend signal in the observed CO_2, at the regional level, is robust to the differing station influence among the models. A comparison of the individual region decadal means utilizing all 13 TransCom 3 models versus the three models identified in Stephens et al. (2007) is shown in Fig. 2 and Table 2. The individual model estimates comprising the S07 three-model mean is also shown.

Between 1980 and 2008 (inclusive), the annual global terrestrial land net flux (NCF) intensified at a rate of -0.057 ± 0.01 PgC yr^{-2}, yielding an increased uptake of -1.65 ± 0.29 PgC over the 29 yr examined here (Fig. 3). This increased uptake was dominated by a decline in the DSNF of -0.037 ± 0.01 PgC yr^{-2} but an intensification of the GSNF (-0.02 ± 0.007 PgC yr^{-2}) also contributed to the annual net flux, indicating that both components contributed to the increased net uptake. As expected, there was a decline in the seasonal amplitude of -0.016 ± 0.013 PgC yr^{-2} (not statistically significant).

The increasing total land net carbon uptake found here is consistent with related findings in recent studies (Cao et al., 2002; Cao et al., 2005; Le Quere et al., 2009; Piao et al., 2009). Sarmiento et al. (2009) also found a trend towards more net carbon uptake on land but the trend was dominated by a shift to greater uptake in 1988/1989 as opposed to a more evenly distributed intensification of uptake over time. Examination of Fig. 3 indicates that such a shift is not found in this study, though the longer time period analysed in Sarmiento et al. (2009) makes it difficult to categorically rule-out a regime-shift in net uptake.

At the broad latitudinal and total land scale (the bottom four rows of Tables 1 and 2), our results suggest intensification of the GSNF in the extratropics coupled with declines in the DSNF, countered by a weakening of GSNF in the tropics. However, the stronger GSNF trends in the northern and particularly southern extratropical land latitudinal aggregates compared to the tropical land result in intensification of the GSNF for the total land and hence, increasing carbon uptake.

Because the inversion results utilized here did not incorporate the seasonality of fossil fuel CO_2, it is worth examining whether or not this could account for seasonal trends estimate estimated here. The only direct interannual, monthly data set available for fossil fuel CO_2 is that reported in Blasing et al. (2005) which reflects emissions from the United States only (approximately 1/5 of the global total). Blasing et al. (2005) note an amplitude decline in the fossil fuel CO_2 emissions though do not estimate the numerical trend. We have calculated the decline in amplitude from this data set, found at http://cdiac.esd.ornl.gov/trends/emis_mon/emis_mon_co2.html, by assigning the months May–August to the GSNF time

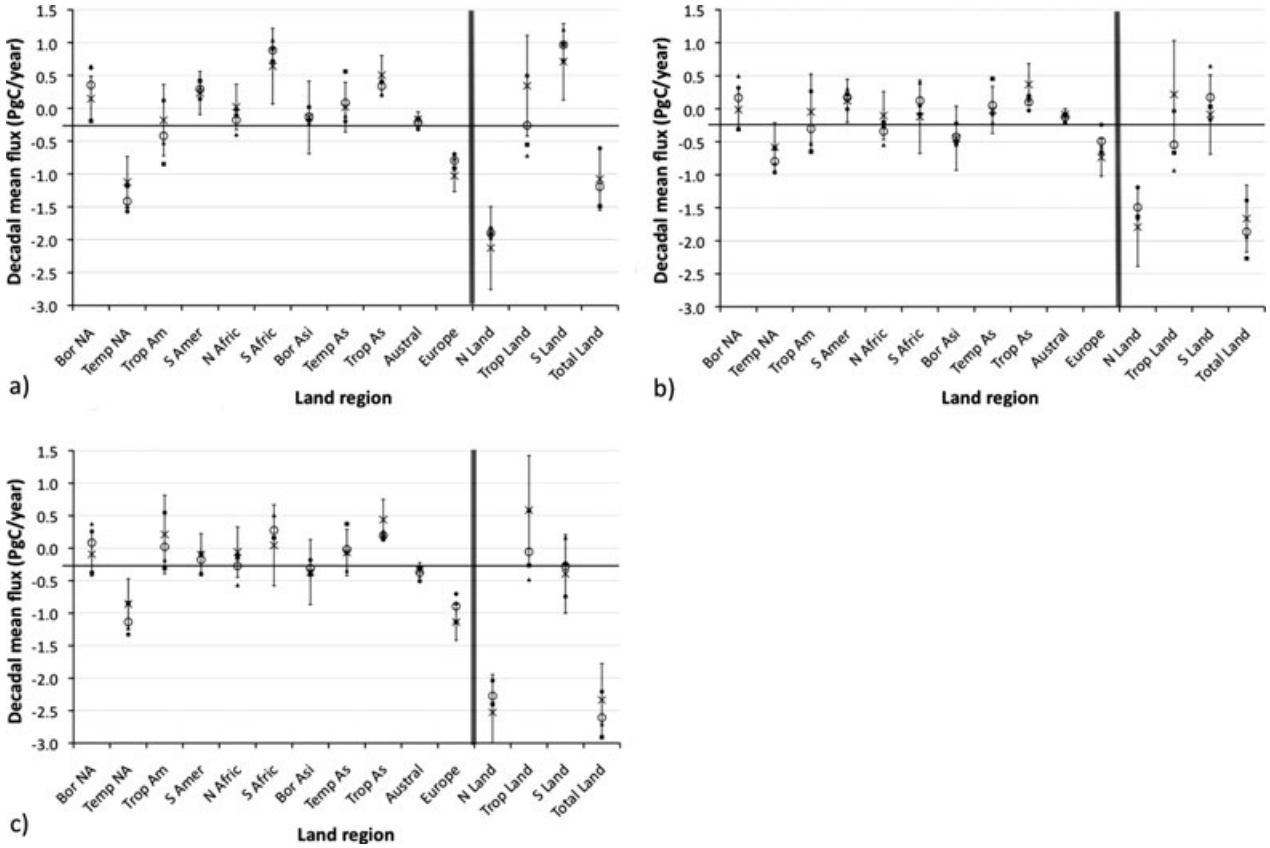

Fig. 2. Comparison of decadal mean net carbon flux for individual land regions. Black cross symbols (X) denote the mean of 13 TransCom 3 models, open circle symbols (O) denote mean of the three S07 TransCom 3 models, individual model estimates within the S07 average are denoted by a filled square, circle and triangle. Vertical error bars represent the total 1σ flux uncertainty (quadrature sum of model spread and the root mean square of individual model posterior uncertainty) associated with the mean of the 13 TransCom 3 models. (a) 1980–1989 mean net carbon flux; (b) 1990–1999 mean net carbon flux; (c) 2000–2008 mean net carbon flux.

period and the remaining months to the DSNF. An average of these two seasonal time periods provides an amplitude decline in the United States of 0.00012 PgC yr^{-2} for the time period spanning 1981–2003. Assuming the remainder of the world had a similar proportional decline, the equivalent amplitude decline would be 0.006 PgC yr^{-2}, more than an order of magnitude smaller than the amplitude decline found in the inverse results.

3.1. Southern land

The drivers of the southern land NCF trend (-0.056 ± 0.009 PgC yr^{-2}) combine intensification of the GSNF (-0.035 ± 0.007 PgC yr^{-2}) and a decline in the DSNF (-0.021 ± 0.005 PgC yr^{-2}). The decadal means indicate that the southern land has changed from a net source of carbon to the atmosphere in the decade of the 1980s to a net sink in the current decade, though uncertainties associated with the long-term means are large. The seasonal amplitude in the southern land carbon exchange is increasing (0.014 ± 0.007 PgC yr^{-2} but not considered statistically significant) due to the greater GSNF intensification.

The southern land result is driven, in large part, by trends in the southern Africa region (NCF trend of -0.032 ± 0.008 PgC yr^{-2}), which shows both intensification of the GSNF and a decline in the DSNF, of roughly equal magnitude. The total change in net flux for the 1980–2008 time period amounts to -0.93 ± 0.2 PgC. Because of the division of Africa along the equator in the TransCom 3 basis function construction, the southern Africa region includes both tropical rainforest and land as far south as 34°S latitude. This makes biological interpretation difficult as this region includes both tropical and extratropical biomes. The northern Africa region, which is considered part of the tropical land aggregate exhibits trends which are an order of magnitude smaller than the southern Africa land region. Hence, trend estimates for the continent, as a whole, are dominated by the southern half. Furthermore, the long-term means show a similar contrast in magnitude. The southern Africa region was estimated as a net source in the decade of the 1980s (0.64 ± 0.58 PgC yr^{-1}) to near-neutral exchange in the current decade

Table 2. TransCom 3 S07[a] model mean decadal mean net exchange for the individual land regions and regional aggregates

	Long-term average NCF (PgC yr^{-1}) & total uncertainty (1σ)		
Biome	1980–1989	1990–1999	2000–2008
Boreal N America	0.36 (0.48)	0.17 (0.43)	0.08 (0.42)
Temperate N America	−1.42 (0.25)	−0.80 (0.23)	−1.14 (0.29)
Tropical America	−0.42 (0.58)	−0.30 (0.58)	0.02 (0.55)
South America	0.29 (0.26)	0.17 (0.27)	−0.18 (0.29)
Northern Africa	−0.18 (0.29)	−0.34 (0.28)	−0.27 (0.34)
Southern Africa	0.89 (0.25)	0.12 (0.32)	0.28 (0.28)
Boreal Asia	−0.13 (0.19)	−0.43 (0.23)	−0.31 (0.18)
Temperate Asia	0.08 (0.46)	0.05 (0.41)	−0.02 (0.41)
Tropical Asia	0.34 (0.20)	0.10 (0.20)	0.20 (0.17)
Australasia	−0.21 (0.11)	−0.12 (0.09)	−0.37 (0.13)
Europe	−0.79 (0.16)	−0.49 (0.24)	−0.90 (0.25)
Northern Land	−1.90 (0.18)	−1.49 (0.31)	−2.28 (0.27)
Tropical Land	−0.26 (0.74)	−0.54 (0.57)	−0.06 (0.65)
Southern Land	0.97 (0.34)	0.17 (0.49)	−0.28 (0.52)
Total Land	−1.19 (0.57)	−1.86 (0.51)	−2.61 (0.44)

Notes: [a]'S07' denotes the three TransCom 3 models (UCI, JMA and TM3) that better represent vertical profiles as described in Stephens et al. (2007).
Uncertainties associated with the long-term decadal means reflect the quadrature sum of the 1σ model spread and the 1σ root mean square of the individual posterior uncertainty.
Details of the uncertainty estimation can be found in previous reports (Gurney et al., 2003).

(0.04 ± 0.62 PgC yr^{-1}). As shown in Fig. 2 and Table 2, the use of the three models identified in the Stephens et al. (2007) study does not alter the decadal means significantly: southern Africa is a source in the 1980s (0.89 ± 0.25 PgC yr^{-1}) shifting to a weaker source in the current decade (0.28 ± 0.28 PgC yr^{-1}). The northern Africa region, by contrast, is a weak sink (not statistically significant) throughout the 29-yr study period.

This result is consistent with recent modelling and inventory studies. For example, Ciais et al. (2009) report model results in which the African continent shifted from a net source of atmospheric CO_2 in the 1980s (0.14 PgC yr^{-1}) to a net sink in the 1990s (−0.15 PgC yr^{-1}). A recent inventory study found a residual net sink in the African tropical forests, which they suggest is close to balancing the deforestation source (Lewis et al., 2009). Emissions from land-use change are uncertain but estimates suggest that little diminishment in net carbon loss due to deforestation and cultivation has occurred through the 1980s and 1990s (DeFries et al., 2002; Williams et al., 2007; Canadell et al., 2009).

The wet phase of the West African Monsoon corresponds to the dry season in the TransCom 3 southern Africa region, which occurs during boreal summer (see Fig. 1b). The dry phase of the West African Monsoon corresponds to the wet season in the TransCom 3 southern Africa region, which occurs during boreal winter. For this region, the DSNF estimated by the net carbon exchange, generally occurs in the dry season and the GSNF generally occurs during the wet season. Hence, the GSNF intensification is occurring during the rainy portion of the year in southern Africa while the decline in DSNF is occurring during the dry portion of the year. One model study has suggested that increased precipitation is the primary driver of increasing African uptake (Ciais et al., 2009) consistent with the GSNF trends found here.

Because the African continent is weakly constrained by atmospheric CO_2 observations, it is worth checking whether or not there are compensatory trend estimates from neighbouring ocean regions, which could be acting as a dipole and hence, indicate an unreliable trend estimate on the land. However, both the South Atlantic (not shown) and the South Indian ocean (not shown) exhibit a negative NCF trend (-0.005 ± 0.0001 PgC yr^{-2} and -0.01 ± 0.001 PgC yr^{-2}, respectively) while the Southern Ocean exhibits a small positive but non-significant NCF trend (0.0025 ± 0.003 PgC yr^{-2}). The latter is consistent with report of a saturation of Southern Ocean carbon uptake over a similar time period (1981–2004) but the trend is smaller than the -0.008 PgC yr^{-2} reported there (LeQuere et al., 2007). This may be due to the inclusion of both Amsterdam Island and Ascension Island in our observational constraint list, which has been reported to alter the trend of net carbon exchange in the Southern Ocean (Law et al., 2008).

3.2. *Tropical land*

The tropical land region aggregate (Tables 1 and 2, third row from bottom), by contrast, shows a positive NCF trend (0.015 ± 0.012 PgC yr^{-2}) driven by a weakening of the GSNF (0.013 ± 0.006 PgC yr^{-2}). Long-term decadal means are sensitive to the model choice as shown in Fig. 2. For the tropical land region aggregate, the average of all 13 models shows a positive net carbon exchange increasing from the 1980s to the 2000s, though diminishing somewhat in the decade of the 1990s. The S07 model average, however, shows net carbon uptake that first strengthens somewhat from the 1980s to the 1990s then substantially weakens from the decade of the 1990s to 2000s. In the 2000s decadal mean, the S07 model mean shows a tropical land region that is essentially carbon neutral while the 13-model average shows a 0.6 PgC yr^{-1} source, driven mostly by tropical Asia (0.44 ± 0.31 PgC yr^{-1}). However, given the uncertainties and the fact that much of the decadal change in the S07 mean is driven by one of the three models included, the difference between the two averaging methods is on the edge of statistical significance.

The tropical land NCF trend is predominantly driven by activity in tropical America which shows a positive NCF trend, estimated at 0.02 ± 0.008 PgC yr^{-2}. This amounts to approximately 0.58 ± 0.23 PgC of additional emissions over the 29 yr of the study. The contributions of the weakening

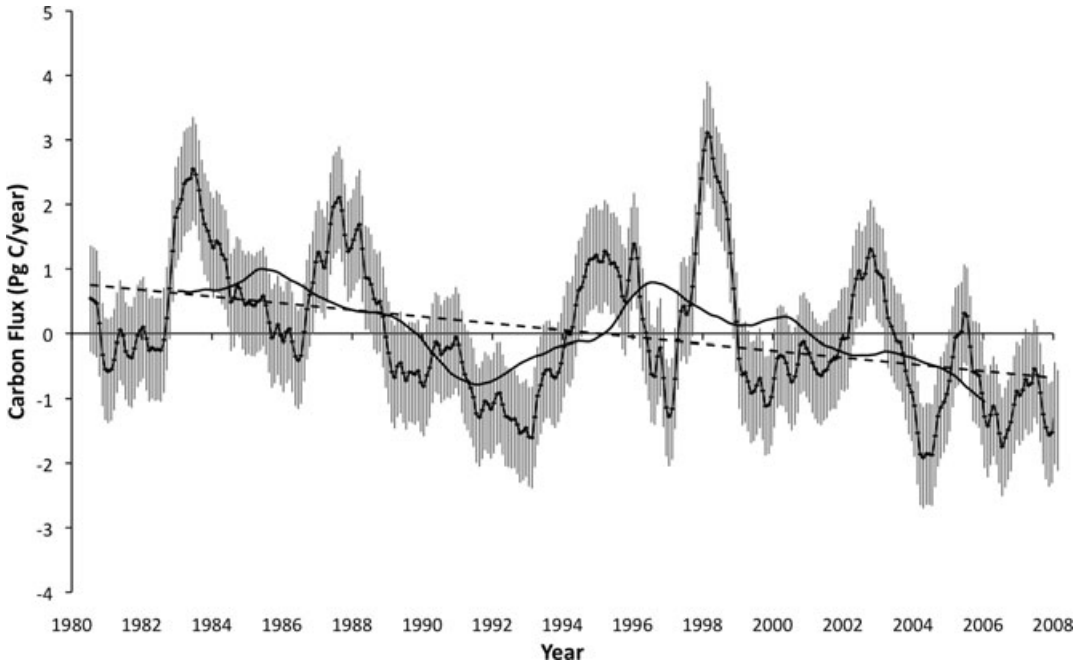

Fig. 3. Terrestrial biosphere net carbon exchange for the 1980–2008 time period. TransCom 3 model mean (13 participating models), monthly deseasonalized total land net carbon flux with long-term mean removed (line with symbols), 5-yr running mean (solid black line) and total 1σ flux uncertainty (quadrature sum of model spread and the root mean square of individual model posterior uncertainty) (grey vertical bars). Dashed black line represents the model mean ordinary least squares fit for the 1980–2008 time period.

GSNF and increasing DSNF were of equal magnitude. Estimation of the long-term flux from tropical America indicates that the region acted as a net sink during the 1980s (-0.18 ± 0.54 PgC yr^{-1}) shifting to a net source in the current decade (0.21 ± 0.60 PgC yr^{-1}). The estimate of NCF when using the three models identified in Stephens et al. (2007) has little impact within the stated uncertainties and would conclude that tropical America was a somewhat larger sink in the 1980s (-0.42 ± 0.58 PgC yr^{-1}) to near-neutral in the current decade (see Fig. 2). However, the individual model estimates show that this is extremely dependent upon the specific model chosen.

Of the potential contributors to net carbon exchange in tropical America, much research has been focused on land-use change. Estimates of land-use change emissions from bookkeeping methods and remote sensing approaches show very different decadal land-use change emissions in tropical America. Although a bookkeeping approach estimates little increase from the 1980s to the 1990s (Houghton, 2003), remote sensing methods estimate a slight increase (a change of roughly 0.1 PgC yr^{-1}) not inconsistent with the 0.13 PgC yr^{-1} change found here (DeFries et al., 2002). A recent model study that attempted to incorporate climate and CO_2 along with land-use change factors, similarly estimate a shift from a net sink to near-neutral carbon exchange (a change of roughly 0.24 PgC yr^{-1}) between the 1980s and 1990s (Piao et al., 2009).

As with the African continent, the interpretation of trends in tropical America is complicated by the definition of the tropical America region within the TransCom 3 experimental setup. The wetter northwestern Amazon is not distinguished from the more seasonal, drier southeastern Amazon. Nevertheless, the GSNF time period for the tropical America region corresponds well to the Amazon-mean dry season which, in turn, has also been shown to correspond to maximum leaf area and months of greatest fire-related emissions (Van Der Werf et al., 2003; Huete et al., 2006; Myneni et al., 2007). An increase in deforestation emissions during the dry season (Van Der Werf et al., 2008) would be consistent with the GSNF trend found here. The impact of drought has been recently reported by Phillips et al. (2009) and they show a reversal of long-term net carbon uptake in Amazonian old-growth forests during the intense 2005 drought. Research has suggested that regional drying and deforestation are internally coupled in a feedback process (Cochrane et al., 1999; Roy and Avissar, 2002; Nepstad et al., 2008). Hence, the temporal coincidence of the GSNF trend, the dry season and deforestation emissions suggest that this positive feedback may be the underlying driving mechanism.

Our finding of an increasing DSNF in tropical America is difficult to deconstruct mechanistically due to the complex potential contervailing fluxes present in the tropical america wet season (which corresponds to our dormant season). For example, eddy covariance measurement in an evergreen, old-growth Amazonian rain forest indicates that the wet season NCF (corresponding to the dormant season here) is positive to the atmosphere owing to greater ecosystem respiration over gross primary production

(Saleska et al., 2007; Hutyra et al., 2007). Unlike extratropical dormant season fluxes, which are dominated by respiration, tropical dormant season fluxes are a mixture of respiration and gross primary production. The increase in DSNF found here could, hence, be due to an increase in ecosystem respiration, a decrease in productivity, or both.

3.3. Northern land

The northern land exhibits a negative NCF trend (-0.016 ± 0.01 PgC yr^{-2}) driven by a combination of GSNF intensification and DSNF decline but the DSNF trend is not significant at the 95% confidence level. The negative NCF trend (increasing carbon uptake) is the result of countervailing trends in the boreal versus temperate North America region. Both boreal North America and boreal Asia show intensification of the GSNF and an increase in the seasonal flux amplitude. Temperate North America, however, exhibits net carbon uptake that is weakening over time. The trend in temperate North America (0.012 ± 0.008 PgC yr^{-2}) is driven by a weakening of the GSNF (0.015 ± 0.007 PgC yr^{-2}). The negative NCF trend in boreal Asia (-0.013 ± 0.007 PgC yr^{-2}) is consistent with results from a recent 21-yr inversion with interannually varying transport in which boreal Asia was found to exhibit increasing uptake over time (-0.017 PgC yr^{-2}) (Chevallier et al., 2010).

Decadal means indicate that the northern land has acted to remove roughly 2 PgC yr^{-1} over the three decades examined here (Fig. 2). Differences between the 13-model mean and the S07 model mean are small and primarily driven by differences in the Europe and Boreal North America regions with the S07 models exhibiting weaker uptake in all three decades. In the case of Europe, the long-term mean estimated by the S07 subset of models is more consistent with bottom-up approaches to net carbon exchange particularly if one accounts for the acknowledged differences in the components that make up inverse versus atmospheric inverse approaches (Janssens et al., 2003). The long-term mean northern land uptake, considering either the 13-model mean or the S07 subset, is driven by carbon removal in temperate North America and Europe.

Numerous studies have demonstrated high latitude increases in NPP based on combinations of in situ observations, terrestrial biosphere models and satellite remote sensing (Myneni et al., 1997; Myneni et al., 2001; Hicke et al., 2002; Lucht et al., 2002; Nemani et al., 2003; Lopatin et al., 2006; Danby and Hik 2007; Sitch et al., 2007; Vuichard et al., 2008) though Goetz et al. (2005) found increasing NPP for tundra and declining NPP for forested regions in boreal North America. The results here show an intensification of the GSNF, which could be either an increase in NPP during the growing season or a weakening of heterotrophic respiration. The lack of a significant trend in the dormant season but a significant and increasing NCF is consistent with these NPP studies but cannot rule out the possibility that there is also a weakening of heterotrophic respiration during the growing season.

Fewer studies have isolated NCF trends and drivers for temperate North America. Those that have, arrive at differing conclusions regarding the trend in temperate North American net uptake (Potter et al., 2003; Angert et al., 2005; Buermann et al., 2007; Piao et al., 2008). Potter et al. (2003) estimated that the North American carbon sink north of 13.5° ranged from -0.2 to -0.3 PgC yr^{-1} throughout the 1980s and 1990s with little discernible trend. However, the disparity may be due to a combination of the limited scope of the net flux calculated in the Potter et al. (2003) study (no land-use change is incorporated) and the differing boundaries. For example, Potter et al. (2003) include boreal and some tropical land in the North America region.

The temperate North American weakening of GSNF, found in this study, is consistent with the decline in LAI found by Piao et al. (2008) which they suggest is due to autumnal warming and the shortening of the period of summer uptake, which is especially pronounced over temperate North America and Europe. We do find a trend towards weakening of European GSNF, however the trend is not statistically significant. The diminished uptake in temperate North America over the time period analysed here is also loosely consistent with studies analysing atmospheric CO_2 observations which suggest weakened uptake due to summer droughts (Angert et al., 2005; Buermann et al., 2007). The Buermann et al. (2007) study utilized the amplitude of atmospheric CO_2 at a single observing site (Mauna Loa) and found growing season amplitude declines in the mid 1980s and starting in the early 1990s onwards, which they associate with temperate North American droughts. However, both the fact that the Buermann et al. (2007) study utilizes a single observing station (compared to regional fluxes optimized from multiple observing locations) and exhibits considerable variability makes confirmation of the trends found in this study open to further investigation.

Similarly, the Angert et al. (2005) study shows declines in net summer uptake from 1990 to 2003, the end of their study period. The preceding 5 yr (1985–1990) show increases in net summer uptake, making the comparison imperfect. Furthermore, the Angert et al. (2005) analysis covers the northern hemisphere $>$ 20°N though it must be noted that the CO_2 observing network utilized in their study has a greater number of stations located in mid-latitudes.

Hence, studies examining only NPP, such as Nemani et al. (2003) may correctly conclude temperate North America increases. However, shortened and weakened net uptake during the growing season may be due to countervailing increases in growing-season heterotrophic respiration, highlighting the importance of the distinction between gross and net fluxes during the growing season.

4. Conclusions

We have computed linear trend values for the seasonal non-fossil land–atmosphere carbon exchange from 1980 to 2008 using results from an atmospheric CO_2 inversion intercomparison which included 13 participating modelling groups. Four indices were created and analysed: GSNF, DSNF, amplitude and annual NCF. We find that the global land carbon sink is intensifying at -0.057 ± 0.01 PgC yr^{-2}, resulting in -1.65 ± 0.29 PgC of additional uptake over the period examined. This increased total land uptake is driven by a decline in the DSNF (-0.04 ± 0.01 PgC yr^{-2}) and intensification of the GSNF (-0.02 ± 0.008 PgC yr^{-2}). Regional analysis shows the dominant role of the southern half of the African continent; intensification of the GSNF (-0.02 ± 0.005 PgC yr^{-2}) and a decline in the DSNF (-0.013 ± 0.004 PgC yr^{-2}) suggest that Africa has shifted from a net carbon source in the 1980s to near-neutral emissions. By contrast, a weakening of the GSNF is found in temperate North America (0.015 ± 0.007 PgC yr^{-2}) and tropical America (0.01 ± 0.005 PgC yr^{-2}).

5. Acknowledgments

This research was supported by DOE on subaward MPC 35WY. We thank the TransCom 3 modelling community for atmospheric CO_2 inversion results and M. Gloor for helpful comments and suggestions.

References

Angert, A., Biraud, S., Bonfils, C., Henning, C. C., Buermann, W. and co-authors. 2005. Drier summers cancel out the CO_2 uptake enhancement induced by warmer springs. *Proc. Nat. Acad. Sci. USA* **102**, 10 823–10 827.

Baker, D., Law, R. M., Gurney, K. R., Denning, A. S., Rayner, P. J., and TransCom 3 modelers, 2006. TransCom 3 inversion intercomparison: impact of transport model errors on the interannual variability of regional CO_2 fluxes, 1988–2003. *Glob. Biogeochem. Cycles* **20**, GB1002, doi:10.1029/2004GB002439.

Blasing, T. J., Broniak, C. T. and Marland, G. 2005. The annual cycle of fossil fuel carbon emissions in the United States. *Tellus* **57B**, 107–115.

Box, G. E. P. and Muller, M. E. 1958. A note on the generation of random normal deviates. *Ann. Math. Statist.* **29**, 610–611.

Bretherton, C. S., Widmann, M., Dymnikov, V. P., Wallace, J. M. and Blade, I. 1999. The effective number of spatial degrees of freedom of a time-varying field. *J. Clim.* **12**, 1990–2009.

Buermann, W., Lintner, B. R., Koven, C. D., Angert, A., Pinzon, J. E. and co-authors. 2007. The changing carbon cycle at Mauna Loa observatory. *Proc. Nat. Acad. Sci. USA* **104**, 4249–4254.

Canadell, J. G., Le Quere, C., Raupach, M. R., Field, C. B., Buitehuis, E. T. and co-authors. 2007. Contributions to accelerating atmospheric CO_2 growth from economic activity, carbon intensity, and efficiency of natural sinks. *Proc. Nat. Acad. Sci. USA* **104**, 18 866–18 870.

Canadell, J. G., Raupach, M. R. and Houghton, R. A. 2009. Anthropogenic CO_2 emissions in Africa. *Biogeosciences* **6**, 463–468.

Cao, M. K., Prince, S. D. and Shugart, H. H. 2002. Effects of interannual climate variability on global terrestrial biospheric CO_2 fluxes. *Glob. Biogeochem. Cycles* **16**, GB1102, doi:10.1029/2001GB001553.

Cao, M., Prince, S. D., Tao, B., Small, J. and Li, K. 2005. Regional pattern and interannual variations in global terrestrial carbon uptake in response to changes in climate and atmospheric CO_2. *Tellus* **57B**, 210–217.

Chevallier, F., Piais, P., Conway, T. J., Aalto, T., Anderson, B. E., and co-authors. 2010. CO_2 surface fluxes at grid point scale estimated from a global 21 year reanalysis of atmospheric measurements. *J. Geophys. Res.* **115**, D21307, doi:10.1029/2010JD013887.

Ciais, P., Piao, S. -L., Cadule, P., Friedlingstein, P. and Chedin, A. 2009. Variability and recent trends in the African terrestrial carbon balance. *Biogeosciences* **6**, 1935–1948.

Cochrane, M. A., Alencar, A., Schulze, M. D., Souza Jr., C. M., Nepstad, D. C., and co-authors. 1999. Positive feedbacks in the fire dynamic of closed canopy tropical forests. *Science* **284**, 1832–1835.

Cox, P. M., Betts, R. A., Jones, C. D., Spall, S. A. and Totterdell, I. J. 2000. Acceleration of global warming due to carbon-cycle feedbacks in a coupled climate model. *Nature* **408**, 184–187.

Danby, R. K. and Hik, V. 2007. Variability, contingency and rapid change in recent subarctic alpine tree line dynamics. *J. Ecol.* **95**, 352–363.

DeFries, R. S., Houghton, R. A., Hansen, M. C., Field, C. B., Skole, D. and co-authors. 2002. Carbon emissions from tropical deforestation and regrowth based on satellite observations for the 1980s and 1990s. *Proc. Nat. Acad. Sci. USA* **99**, 14 256–14 261.

Denman K.L., Brasseur, G., Chidthaisong, A., Ciais, P., Cox, P.M. and co-author. 2007. Couplings between changes in the climate system and biogeochemistry. In: *Climate Change 2007: The Physical Science Basis*. Contribution of Working Group I to the Fourth Assessment Report of the Intergovernmental Panel on Climate Change (eds S. Solomon, D. Qin, M. Manning, Z. Chen, M. Marquis, K.B. Averyt, M. Tignor, and H.L. Miller). Cambridge University Press, Cambridge, United Kingdom and New York, NY, USA.

Engelen R. J., Denning, A. S., Gurney K. R., and TransCom 3 modelers. 2002. On error estimation in atmospheric CO_2 inversions. *J. Geophys. Res.* **107**, 4635, doi:10.1029/2002JD002195.

Enting I. 2002. *Inverse Problems in Atmospheric Constituent Transport*, Cambridge University Press, Cambridge, UK.

Friedlingstein P., Cox, P., Betts, R., Bopp, L., Von Bloh, W. and co-authors. 2006. Climate-carbon cycle feedback analysis, results from the C4MIP model intercomparison. *J. Clim.* **19**, 3337–3353.

GLOBALVIEW-CO_2. 2009. *Cooperative Atmospheric Data Integration Project: Carbon Dioxide*. CD-ROM, NOAA ESRL, Boulder, Colorado.

Gloor M., Sarmiento, J. and Gruber, N. 2010. What can be learned about carbon cycle climate feedbacks from the CO2 airborne fraction?. *Atmos. Chem. Phys.* **10**, 7739–7751.

Goetz S. J., Bunn, A. G., Fiske, G. J. and Houghton, R. A. 2005. Satellite-observed photosynthetic trends across boreal North America associated with climate and fire disturbance. *Proc. Nat. Acad. Sci. USA* **102**, 13 521–13 525.

Gurney K. R., Law, R. M., Denning, A. S., Rayner, P. J., Baker, D. and co-authors. 2002. Towards robust regional estimates of CO_2 sources and sinks using atmospheric transport models. *Nature* **415**, 626–630.

Gurney K. R., Law, R. M., Denning, A. S., Rayner, P. J., Baker, D. and co-author. 2003. TransCom 3 CO_2 inversion intercomparison: 1.

Annual mean control results and sensitivity to transport and prior flux information. *Tellus* **55B**, 555–579.

Gurney, K. R., Law, R. M., Denning, A. S., Rayner, P. J., Pak, B., and the TransCom 3 L2 modelers. 2004. Transcom 3 inversion intercomparison: control results for the estimation of seasonal carbon sources and sinks. *Glob. Biogeochem. Cycles*, **18**, GB1010, doi:10.1029/2003GB002111.

Gurney, K. R., Baker, D., Rayner, P., Denning, A. S. and TransCom 3 L2 modelers. 2008. Interannual variations in continental-scale net carbon exchange and sensitivity to observing networks estimated from atmospheric CO_2 inversions for the period 1980 to 2005. *Glob. Biogeochem. Cycles* **22**, GB3025 doi:10.1029/2007GB003082.

Hicke, J. A., Asner, G. P., Randerson, J. T., Tucker, C., Los, S. and co-authors. 2002. Trends in North American net primary productivity derived from satellite observations, 1982–1998. *Glob. Biogeochem. Cycles* **16**, doi:10.1029/2001GB001550.

Houghton, R. A. 2003. Revised estimates of the annual net flux of carbon to the atmosphere from changes in land use and land management 1850–2000. *Tellus* **55B**, 378–390.

Huete A. R., Didan, K., Shimabukuro, Y., Ratana, P., Saleska, S. R. and co-authors. 2006. Amazon rainforests green-up with sunlight in dry season. *Geophys. Res. Lett.* **33**, doi:10.1029/2005GL025583.

Hutyra L. R., Munger, J. W., Saleska, S. R., Gottlieb, E., Daube, B. C. and co-authors. 2007. Seasonal controls on the exchange of carbon and water in an Amazonian rain forest. *J. Geophys. Res.* **112**, G03008 doi:10.1029/2006JG000365.

Janssens I. A., Freibauer, A., Ciais, P., Smith, P., Nabuurs, G.-J., Folberth, G., Schlamadinger, B., Hutjes, R. W. A., Ceulemans, R., Schulze, E.-D., Valentini, R. and Dolman, J. 2003. Europe's Terrestrial Biosphere Absorbs 7 to 12% of European Anthropogenic CO2 Emissions. *Science* **300**, 1538–1542.

Knorr, W. 2009. Is the airborne fraction of anthropogenic CO_2 emissions increasing? *Geophys. Res. Lett.* **36**, doi:10.1029/2009GL040613.

Law, R.M., Matear, R. J. and Francey, R. J. 2008. Comment on "Saturation of the southern ocean CO_2 sink due to recent climate change". *Science* **319**, 570, doi:10.1126/science.1149077.

Le Quere, C., Rodenbeck, C., Buitenhuis, E. T., Conway, T. J., Langenfelds, R. and co-authors. 2007. Saturation of the southern ocean CO_2 sink due to recent climate change. *Science* **316**, 1735–1738.

Le Quere C., Raupach, M. R., Canadell, J. G., Marland, G., Bopp, L. and co-authors. 2009. Trends in the sources and sinks of carbon dioxide. *Nature Geosci.* **2**, 831–836.

Lewis, S. L., Lopez-Gonzalez, G., Sonke, B., Affum-Baffoe, K., Baker, T. R. and co-authors. 2009. Increasing carbon storage in intact African tropical forests. *Nature* **457**, 1003–1006.

Lopatin, E., Kolström, T. and Spiecker, H. 2006. Determination of forest growth trends in Komi Republic (northwestern Russia): combination of tree-ring analysis and remote sensing data. *Boreal Env. Res.* **11**, 341–353.

Lucht W., Prentice, I. C., Myneni, R. B., Sitch, S., Friedlingstein, P. and co-authors. 2002. Climatic control of the high-latitude vegetation greening trend and Pinatubo effect. *Science* **296**, 1687–1689.

Myneni R. B., Keeling, C. D., Tucker, C. J., Asrar, G. and Nemani, R. R. 1997. Increased plant growth in the northern hemisphere high latitudes from 1981 to 1991. *Nature* **366**, 698–702.

Myneni, R. B., Dong, J., Tucker, C. J., Kaufmann, R. K., Kauppi, P. E. and co-authors. 2001. A large carbon sink in the woody biomass of Northern forests. *Proc. Nat. Acad. Sci. USA.* **98**, 14 784–14 789.

Myneni, R. B., Yang, W., Nemanic, R. R., Huete, A. R., Dickinson, R. E. and co-authors. 2007. Large seasonal swings in leaf area of Amazon rainforests. *Proc. Nat. Acad. Sci. USA* **104**, 4720–4823.

Nemani R. R., Keeling, C. D., Hashimoto, H., Jolly, W. M., Piper, S. C. and co-authors. 2003. Climate driven increases in global terrestrial net primary production from 1982 to 1999. *Science* **300**, 1560–1563.

Nepstad, D. C., Stickler, C. M., Soares-Filho, B. and Merry F. 2008. Interactions among Amazon land use, forests and climate: prospects for a near-term forest tipping point. *Phil. Trans. R. Soc. B.* **363**,1737–1746.

Peylin, P., Bousquet, P., Le Quere, C., Sitch, S., Friedlingstein, P. and co-authors. 2005. Multiple constraints on regional CO_2 flux over land and oceans. *Glob. Biogeochem. Cycles* **19**, doi:10.1029/2003GB002214.

Phillips, O. L., 2009. Drought sensitivity of the Amazon rainforest. *Science* **323**, 1344, doi: 10.1126/science.1164033

Piao S., Ciais, P., Friedlingstein, P., Peylin, P., Reichstein, M. and co-authors. 2008. Net carbon dioxide losses of northern ecosystems in response to autumn warming. *Nature* **451**, 49–53.

Piao, S., Ciais, P., Friedlingstein, P., de Noblet-Ducoudre´, N., Cadule, P. and co-authors. 2009. Spatiotemporal patterns of terrestrial carbon cycle during the 20th century. *Glob. Biogeochem. Cycles* **23**, doi:10.1029/2008GB003339.

Potter, C. S., Klooster, S., Myneni, R., Genovese, V., Tan, P. and co-authors. 2003. Continental-scale comparisons of terrestrial carbon sinks estimated from satellite data and ecosystem modeling 1982–1998. *Glob. Planet. Change* **39**, 201–213.

Randerson, J. T., Thompson, M. V., Conway, T. J., Fung, I. Y. and Field, C. B. 1997. The contribution of terrestrial sources and sinks to trends in the seasonal cycle of atmospheric carbon dioxide. *Glob. Biogeochem. Cyc.* **11**, 535–560.

Raupach, M. R., Canadell, J. G. and Le Quere. C. 2008. Anthropogenic and biophysical contributions to increasing atmospheric CO_2 growth rate and airborne fraction. *Biogeosciences* **5**, 1601–1613.

Rödenbeck C., Howeling, S., Gloor, M. and Heimann, M. 2003. CO_2 flux history 1982–2001 inferred from atmospheric data using a global inversion of atmospheric transport. *Atmos. Chem. Phys. Discuss.* **3**, 2575–2659.

Roy, S. B. and Avissar, R. 2002. Impact of land use/land cover change on regional hydrometeorology in Amazonia. *J. Geophys. Res.* **107**, doi:10.1029/2000JD000266.

Saleska, S. R., Didan, K., Huete, A. R. and da Rocha, H. R. 2007. Amazon forests green-up during 2005 drought. *Science* **318**, doi:10.1126/science.1146663.

Sarmiento, J., Gloor, M., Gruber, N., Beaulieu, C., Jacobson, A.R. and co-author. 2009. Trends and regional distributions of land and ocean carbon sinks. *Biogeosci. Discuss.* **6**, 10 583–10 624.

Schaefer K., Denning, A. S., Suits, N., Kaduk, J., Baker, I. and co-authors. 2002. Effect of climate on interannual variability of terrestrial CO_2 fluxes. *Glob. Biogeochem. Cycles* **16**, doi:10.1029/2002GB001928.

Sitch, S., McGuire, D., Kimball, J., Gedney, N., Gamon, J. and co-authors. 2007. Assessing the carbon balance of circumpolar arctic tundra using remote sensing and process modeling. *Ecol. App.* **17**, 213–234.

Sitch S., Huntingford, C., Gedney, N., Levy, P. E., Lomas, M. and co-authors. 2008. Evaluation of the terrestrial carbon cycle, future

plant geography and climate-carbon cycle feedbacks using five Dynamic Global Vegetation Models (DGVMs). *Glob. Change Biol.* **14**, 2015–1039.

Stephens B. B., Gurney, K. R., Tans, P. P., Sweeney, C., Peters, W. and co-authors. 2007. Weak northern and strong tropical land carbon uptake from vertical profiles of atmospheric CO_2. *Science* **316**, 1732–1735.

Tans, P. P., Fung, I. Y. and Takahashi, T. 1990. Observational constraints on the global atmospheric CO_2 budget. *Science* **247**, 1431–1438.

Van Der Werf, G., Randerson, J.T., Collatz, J. and Giglio, L. 2003. Carbon emissions from fires in tropical and subtropical ecosystems. *Glob. Change Biology* **9**, 547–562.

Van Der Werf, G., Randerson, J. T., Giglio, L., Gobron, N. and Dolman, A. J. 2008. Climate controls on the variability of fires in the tropics and subtropics. *Glob. Biogeochem. Cycles* **22**, GB3028, doi:10.1029/2007GB003122.

Vuichard, N., Ciais, P., Belelli, L., Smith, P. and Valentini, R. 2008. Carbon sequestration due to the abandonment of agriculture in the former USSR since 1990. *Glob. Biogeochem. Cycles* **22**, doi:10.1029/2008GB003212.

Williams C. A., Hanan, N. P., Neff, J. C., Scholes, R. J., Berry, J. A. and co-authors. 2007. Africa and the global carbon cycle. *Carbon Bal. Mngmnt.* **2**, doi:10.1186/1750-0680-2-3.